Spin Resonance of Pd and Pt in Silicon

H. H. WOODBURY AND G. W. LUDWIG
General Electric Research Laboratory, Schenectady, New York
(Received November 28, 1961)

The transition metals Pd and Pt usually occur in diamagnetic form. However, in silicon both Pd and Pt act as acceptor impurities; the ions Pd^- and Pt^- are paramagnetic and have been studied by electron spin resonance. Both ions have a [001] and two mutually perpendicular [110] axes as principal axes of the g tensor. Hyperfine interaction with Pd^{105}, Pt^{195}, and Si^{29} has been detected and studied. In particular, Pd^{105} shows a strong quadrupolar interaction. The spectra are discussed in terms of models in which the ions are distorted from the normal substitutional site along a cubic direction. A second spectrum, which may represent a defect pair, has been observed for Pt.

I. INTRODUCTION

IN the course of a study of impurities in semiconductors, spin resonance has been observed for ions of palladium and platinum in silicon.[1] The results on these ions are of particular interest for several reasons: (1) This is one of the first observations of spin resonance for Pd and Pt in any host lattice[2]; the common charge states are +4 and +6, which are diamagnetic.[3] (2) Spin resonance of transition metal ions of the 4*d* and 5*d* groups has not been reported previously in a semiconductor, where one anticipates that effects of covalency[4] will be important. (3) Pd and Pt occupy distorted sites in the silicon lattice, analogous to those occupied by Ni in Ge.[5] Other transition metal impurities in Si and Ge occupy symmetrical sites.[6–8]

Using techniques described in connection with studies of other transition metal ions,[6] Pd and Pt were introduced by diffusion into silicon containing shallow donors, shallow acceptors, or no intentionally added impurities. In crystals containing shallow donors one resonant center was found for Pd, while two centers, designated I and II, were found for Pt. The Pt(I) center was the more abundant of the Pt centers: Its spectrum is anisotropic and has been detected only at low temperatures ($T \lesssim 12$°K). The Pt(II) spectrum, on the other hand, was observed at 20°K and higher, and varied in intensity from sample to sample. No spectra were detected in samples containing Pd or Pt but no donor impurities.

The intensity of the Pd, Pt, and shallow donor resonance signals were measured as a function of donor concentration. The results showed that Pd and Pt act as acceptor impurities, and have solubilities between 1 and $4\times10^{16}/cm^3$ at 1300°C. The intensity of the resonance signals from these centers was unaffected by donor concentrations in excess of this solubility. Thus, we conclude that the dominant resonant centers are Pd^- and $Pt(I)^-$, and that more negative charge states of Pd and Pt(I) are not formed.

Radiotracer studies by Carlson[9] indicated a solubility $\sim3\times10^{16}/cm^3$ for Pd at 1200°C. Carlson[9] also detected an electrical level at about 0.34 ev from the valence band in Pd-doped samples. This level was not definitely attributed to Pd since contamination of the samples with Au or Zn, which have levels near that value, could not be ruled out. The present spin resonance results are consistent with Carlson's solubility measurement, and make it appear likely that the 0.34-ev electrical level is the Pd acceptor level.

Electrical data on Pt are less definitive, although two levels, at about 0.34 ev and 0.45 ev from the valence band, were observed.[9] The latter level was not found consistently and may be associated with the Pt(II) center.

Samples were examined in a spin resonance spectrometer, described elsewhere,[6] which operates at about 14 kMc/sec. The electron-nuclear double-resonance technique[10] was also found helpful.

The resonance pattern for the Pd^- center indicates that there are six geometrically nonequivalent sites, which give rise to six independent spectra. Each spectrum has a [001] direction and two mutually perpendicular [110] directions as the principal axes of the g tensor. Moreover, there is resolved hyperfine interaction with the 4.7% abundant isotope Si^{29} occupying two nearby sites. The relative orientation of the axes of the g tensor and the axes of the Si^{29} hyperfine interaction is illustrated in Fig. 1(a). The anisotropy of the spectrum of the Pd^- center indicates that the ion does not occupy an isolated symmetrical lattice position. One geometry for the center which is consistent with the principal axes of Fig. 1(a) is illustrated in Fig. 1(b).

[1] H. H. Woodbury and G. W. Ludwig, Bull. Am. Phys. Soc. **5**, 158 (1960).
[2] Recently, spin resonance of Pt has also been detected in Al_2O_3. See S. Geschwind and J. P. Remeika, J. Appl. Phys. **33**, 370 (1962).
[3] J. H. E. Griffiths, J. Owen, and I. M. Ward, Proc. Roy. Soc. (London) **A219**, 526 (1953).
[4] K. W. H. Stevens, Proc. Roy. Soc. (London) **A219**, 542 (1953).
[5] G. W. Ludwig and H. H. Woodbury, Phys. Rev. **113**, 1014 (1959).
[6] H. H. Woodbury and G. W. Ludwig, Phys. Rev. **117**, 102 (1960).
[7] G. W. Ludwig, H. H. Woodbury, and F. S. Ham (to be published); G. W. Ludwig and H. H. Woodbury, *Solid-State Physics*, edited by F. Seitz and D. Turnbull (Academic Press, Inc., New York, 1962), Vol. 13.
[8] G. D. Watkins, Bull. Am. Phys. Soc. **2**, 345 (1957).
[9] R. O. Carlson, Report No. P-128, General Electric Research Laboratory, 1957 (unpublished).
[10] G. Feher, Phys. Rev. **114**, 1219 (1959).

It is believed that the Pd^- is not associated with another defect, but rather distorts from a substitutional position along a cubic axis.[11]

The resonance pattern of the $Pt(I)^-$ center can also be interpreted in terms of six geometrically nonequivalent sites; Fig. 1(a) again gives typical principal axes, while Fig. 1(b) shows a possible geometrical arrangement. In contrast, the Pt(II) center shows four distinct sites, each having a spectrum displaying axial symmetry about a [111] direction.

The spin Hamiltonian appropriate to the Pd^-, $Pt(I)^-$, and Pt(II) centers in silicon is discussed in Sec. II, while the experimental results are presented in Secs. III and IV, and are discussed in Sec. V.

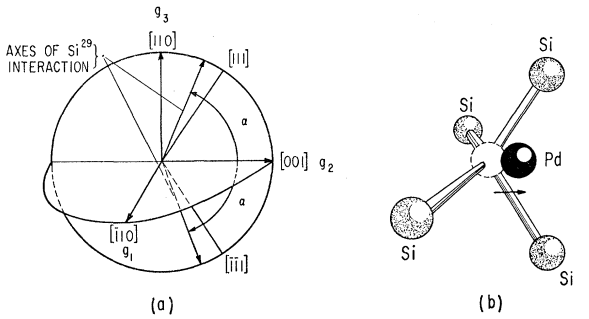

FIG. 1. (a) Principal axes for the g tensor and hyperfine interactions of the $(Pd^{105})^-$ center in silicon. (b) A geometrical model for the Pd^- center consistent with the principal axes shown in (a).

II. THE SPIN HAMILTONIAN

The spin Hamiltonian for a center of rhombic symmetry having $S=\frac{1}{2}$ is

$$\mathcal{H}=\beta\mathbf{S}\cdot\mathbf{g}\cdot\mathbf{H}+\mathbf{S}\cdot\mathbf{A}\cdot\mathbf{I}+\mathbf{I}\cdot\mathbf{P}\cdot\mathbf{I}-g_N\beta_N\mathbf{H}\cdot\mathbf{I}+\sum_k[\mathbf{S}\cdot\mathbf{T}_k\cdot\mathbf{I}_k-(g_N)_k\beta_N\mathbf{H}\cdot\mathbf{I}_k]. \quad (1)$$

The first term in (1) describes the interaction of the unpaired electron with the applied magnetic field; the second, third, and fourth terms represent hyperfine interactions involving the impurity nucleus; and the remaining terms give the hyperfine interactions involving Si^{29} nuclei of the host lattice. In general $\mathbf{g}$, $\mathbf{A}$, $\mathbf{P}$, and the $\mathbf{T}_k$ are second order tensors, and $\mathbf{g}$, $\mathbf{A}$, and $\mathbf{P}$ have the same principal axes. Neglecting for the moment the quadrupolar and Si^{29} interactions, the energy levels $W_{M,m}$ are approximately

$$W_{M,m}=g\beta HM+KMm-g_N\beta_N Hm, \quad (2)$$

with

$$g^2=(g_1\cos\theta_1)^2+(g_2\cos\theta_2)^2+(g_3\cos\theta_3)^2,$$

$$K^2g^2=(A_1g_1\cos\theta_1)^2+(A_2g_2\cos\theta_2)^2+(A_3g_3\cos\theta_3)^2. \quad (3)$$

The parameters g_i and A_i are the principal values of $\mathbf{g}$ and $\mathbf{A}$, respectively, and the θ_i are the angles between $\mathbf{H}$ and the principal axes.

For axial symmetry (3) reduces to

$$g^2=(g_\parallel\cos\theta)^2+(g_\perp\sin\theta)^2,$$
$$K^2g^2=(Ag_\parallel\cos\theta)^2+(Bg_\perp\sin\theta)^2. \quad (4)$$

Here $g_\parallel$ and $g_\perp$ are the g values parallel to and perpendicular to the axis of symmetry; A and B are hyperfine interaction constants similarly defined; and θ is measured between $\mathbf{H}$ and the symmetry axis. Thus, the $M=+\frac{1}{2}$ to $-\frac{1}{2}$, $\Delta m=0$ transitions are given by

$$h\nu=g\beta H+Km. \quad (5)$$

The spectra of the Pd^- and $Pt(I)^-$ centers are conveniently analyzed with $\mathbf{H}$ in a (110) plane. Under these conditions the g factor for the line which arises from centers oriented as in Fig. 1(a) is

$$g^2=(g_1\cos\varphi)^2+(g_2\sin\varphi)^2, \quad (6)$$

where φ is measured from the [110] direction. The transition resulting from this orientation is referred to below as line B. Other centers have differently oriented g tensors resulting in a six-line spectrum for arbitrary direction of magnetic field. In particular, the line which we call line A has the same g tensor except that the roles of g_1 and g_3 are interchanged; Its g factor is given by

$$g^2=(g_3\cos\varphi)^2+(g_2\sin\varphi)^2. \quad (7)$$

The spectrum of the Pd^- center displays a large axially symmetric hyperfine interaction with Si^{29} occupying two positions in the plane defined by the 2 and 3 axes of the center. The interactions with Si^{29} are equal in magnitude and differ only in the orientation of the symmetry axis. To describe these interactions for the centers which give rise to line B, Eq. (2) must be augmented by[12]

$$(m_{Si}M/2g)[T_\parallel^2(g_2\sin\varphi\cos\alpha)^2+T_\perp^2(g_1^2\cos^2\varphi+g_2^2\sin^2\varphi\sin^2\alpha)]^{\frac{1}{2}}-m_{Si}(g_N)_{Si}\beta_N H. \quad (8)$$

Here, α is the angle between the 2 axis and the axis of the hyperfine interaction, and $T_\parallel$ and $T_\perp$ are hyperfine interaction constants. In the case of line A, Eq. (2) is augmented by[12]

$$(m_{Si}M/2g)[T_\parallel^2(g_3\cos\varphi\sin\alpha+g_2\sin\varphi\cos\alpha)^2+T_\perp^2(g_3\cos\varphi\cos\alpha-g_2\sin\varphi\sin\alpha)^2]^{\frac{1}{2}}-m_{Si}(g_N)_{Si}\beta_N H. \quad (9)$$

The quantity $\sin\alpha$ differs in sign for the two positions for Si^{29}. For line A this results in two sets of Si^{29} lines.

III. THE SPECTRUM OF THE Pd^- CENTER

The angular dependence of the g factor of the Pd^- center is shown in Fig. 2. For $\mathbf{H}$ in the (110) plane

[11] This model is the one adopted for the Ni^- center in Ge (see reference 5). The spectra of the Ni^- center in Ge and the Pd^- center in Si are very similar.

[12] The general procedure for this calculation is briefly outlined in reference 5. It is noted that Eq. (2) and Fig. 6 in reference 5 are inaccurate [compare with Eq. (9) and Fig. 3 below].

TABLE I. Resonance parameters for Pd^{105} and Pt^{195} in Si. The components of A, P, and T are expressed in 10^{-4} cm^{-1}.

Center	Typical axes	g	$\|A\|$	P	Typical axes for T	$\|T\|$
Pd^-	[$\bar{1}$10]	1.9190	12.2	±5.3	Fig. 1(a)	$T_{\parallel}=50.1$
	[001]	2.0544	6.0	∓4.7	with $\alpha\simeq60°$	$T_{\perp}=35.7$
	[110]	1.9715	(36)	∓0.6		
Pt(I)$^-$	[$\bar{1}$10]	1.4266	184.2		uncertain	($T_{\parallel}=38$)
	[001]	2.0789	127.0			($T_{\perp}=25$)
	[110]	1.3867	147.0			
Pt(II)	$\parallel$ to [111]	2.021	156			
	$\perp$ to [111]	2.126	62			

there are four lines, each of which is split by hyperfine interactions. The principal values of the g tensor, given in Table I, were obtained from lines B and A, which are described by (6) and (7), respectively.

The hyperfine interaction with Si^{29} was studied both by spin resonance and by electron-nuclear double resonance. The interaction was found to be large for Si^{29} occupying two positions in the 2–3 plane, as discussed in II. The interaction for lines A and B is plotted in Fig. 3 as measured by double resonance. It is noted that the axes for the interaction depart from [111] directions, the normal nearest neighbor directions, by about 5°. The sense of the distortion is that the angle between the two Si^{29} axes is increased from the normal tetrahedral value (109.5°). The values $T_{\parallel}$ and $T_{\perp}$ of Table I were computed from line A.

Hyperfine interaction with Pd^{105}, a 22% abundant isotope having $I=\frac{5}{2}$, was also observed. The hyperfine structure shows several unusual features for certain orientations of **H**. The hyperfine spacing is greater at the ends of the pattern than in the middle; at other orientations hyperfine lines cross, and forbidden hyperfine transitions can be detected. The interaction was studied by spin resonance and electron-nuclear double resonance using samples doped with Pd enriched in the isotope Pd^{105}. The observations can be accounted for in terms of a quadrupolar interaction of Pd^{105}.

The case in which the nuclear quadrupolar interaction is large compared to its magnetic interactions

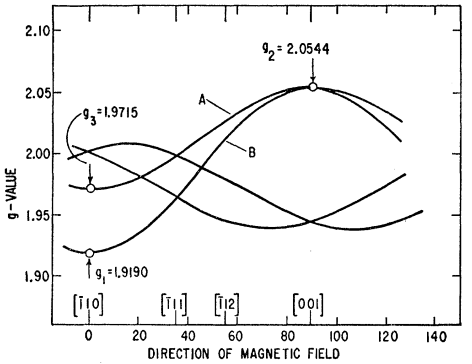

FIG. 2. The g factor of the Pd^- center with the magnetic field in the (110) plane. Lines A and B are described by (7) and (6), respectively.

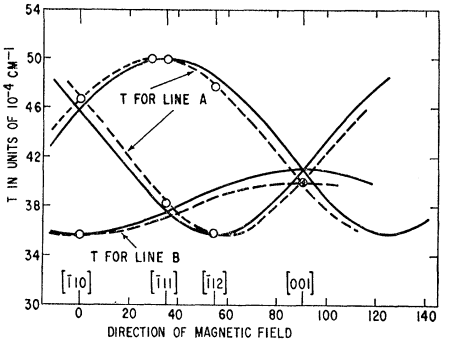

FIG. 3. The hyperfine interaction of the Pd^- center with Si^{29}. The dashed curves represent (8) and (9) for $\alpha=60°$ [see Fig. 1(a)], which gives the best fit to the experimental data, while the solid curves correspond to $\alpha=54.7°$. The latter value would apply if the axes of the hyperfine interaction were [111] directions.

has been treated by Cohen[13] for $I=\frac{5}{2}$ in connection with the Zeeman splitting of nuclear quadrupole resonance lines.[14] The present spin resonance case is somewhat different from the one treated by Cohen. Here, the major magnetic interaction of the nucleus is with the hyperfine field, which has the direction cosines

$$\cos\theta_i'=(A_i g_i\cos\theta_i)/Kg;\quad i=1,\ 2,\ 3. \tag{10}$$

Neglecting the direct interaction of the nucleus with the external field, assuming $|P_3|<|P_2|<|P_1|$, and using Cohen's Eq. (9), our Eq. (2) becomes

$$W_{M,\pm m}=g\beta HM+E^0P_1\mp KM[A\cos^2\theta_1' +\tfrac{1}{4}(B-2C)\sin^2\theta_1'+C\cos^2\theta_3']^{\frac{1}{2}}, \tag{11}$$

where E^0P_1 gives the nuclear quadrupolar interaction in zero magnetic field. The coefficients E^0, A, B, and C are given in Table II of Cohen's article[13] as a function of m and the asymmetry parameter $\eta=(P_3-P_2)/P_1$.

The magnitudes of the hyperfine interaction parameters A_1 and A_2 and the P_i of Table I were estimated using (11) and electron-nuclear double-resonance measurements on line B; the signs could not be determined. As a check, the hyperfine splitting of line B as determined by spin resonance was compared with the predictions of (11), as shown in Fig. 4. Since (11) accounts for the double-resonance and spin-resonance measurements, one has some confidence in the calculated parameters despite the comparable size of the quadrupolar and magnetic hyperfine interactions.

The hyperfine pattern for line A with **H** along the 3 axis was spread over 82 gauss and showed many forbidden transitions. In the approximation that the quadrupolar interaction is large compared to the magnetic interaction and using the asymmetry parameter determined from line B, one finds that the outermost lines correspond to $\Delta M=\pm1$, $m=\pm\frac{3}{2}$ transitions with

[13] M. H. Cohen, Phys. Rev. **96**, 1278 (1954).

[14] T. P. Das and E. L. Hahn, in *Solid-State Physics*, edited by F. Seitz and D. Turnbull (Academic Press, Inc., New York, 1958), Suppl. 1.

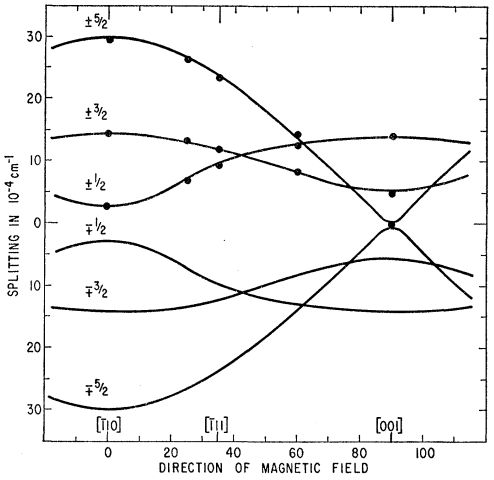

FIG. 4. The Pd^{105} hyperfine splitting of line B as a function of the direction of H. The experimental points were obtained by spin resonance, while the curves were derived from (11).

$A_3=36\times10^{-4}$ cm^{-1}. Since (11) does not accurately account for the other hyperfine lines, this value for A_3 should be considered very tentative.

The temperature dependence of the spectrum of the Pd^- center was also examined. When the sample is warmed above 20.4°K the lines broaden and eventually disappear. No motional averaging of the g tensor was observed, contrary to the results on Ni in Ge[5]. Apparently spin-lattice relaxation broadens the resonance transitions of different Pd^- sites before the re-orientation rate of the sites becomes comparable to their frequency differences.

Crystals containing Pd^- were subjected to a uniaxial stress, destroying the tetrahedral symmetry of the lattice and establishing a preferred orientation for the centers.[15] In particular, for a stress along the [110] direction the sites re-orient, lowering the intensity of lines A and B, particularly A. This effect has not been explained.

IV. SPECTRA OF THE Pt(I)$^-$ AND Pt(II) CENTERS

The g tensor of the Pt(I)$^-$ center, shown in Fig. 5, displays the same principal axes as those for the Pd^- center; It is, however, much more anisotropic. Hyperfine interaction with Si^{29} was observed. Assuming that the structure on lines A and B is analogous to that studied for the Pd^- center, one calculates $T_{\parallel}$ and $T_{\perp}$ as given in Table I from measurements in the [110] and [001] directions. However, the structure was not well resolved nor understood at all angles: $T_{\parallel}$, $T_{\perp}$, and the axes of the hyperfine interaction are considered tentative. Evidence of weaker Si^{29} interaction ($T\sim10\times10^{-4}$ cm^{-1}) was also found. The hyperfine interaction with the 34% abundant isotope Pt^{195} having $I=\frac{1}{2}$ was studied. Resonance parameters are given in Table I. As the sample temperature is raised above 12°K, the spectrum broadens and then disappears. The Pt(I)$^-$ center behaves similarly to the Pd^- center upon application of a uniaxial stress.

The spectrum of the Pt(II) center shows that there are four types of sites, each described by (4) and (5) with the symmetry axis a different one of the four [111] directions. Parameters are summarized in Table I. The spectrum is detectable at 20°K and below. It is insensitive to uniaxial stress.

When samples in which the Pt(I) and Pt(II) centers were nearly or completely compensated with Sb were held at 10°K and irradiated with incandescent light, the spectra due to both centers disappeared, while the Sb resonance increased in intensity. Moreover, when the light was turned off, the spectrum of the Pt(I)$^-$ center reappeared immediately, while the spectrum of the Pt(II) center reappeared only after the sample was warmed to 20°K. We conclude that both centers act as hole traps. The long trapping time associated with the Pt(II) center at 10°K suggests that it may be a double acceptor,[16] the resonant form being the doubly charged state.

The intensity of the spectrum of the Pt(II) center varied from sample to sample, and showed some correlation with the oxygen content. Thus, this center may represent Pt associated with oxygen.

V. DISCUSSION

Several observations indicate that Pd and Pt are substitutional in Si. First, the resonant centers are quite stable, as one expects if the impurities are substitutional; on the other hand, centers involving interstitial transition metals are unstable at room temperature.[6,7] Second, comparing Pd and Pt with their 3d analog, Ni, both elements show a spectrum analogous to that of substitutional Ni^- in Ge. In silicon,

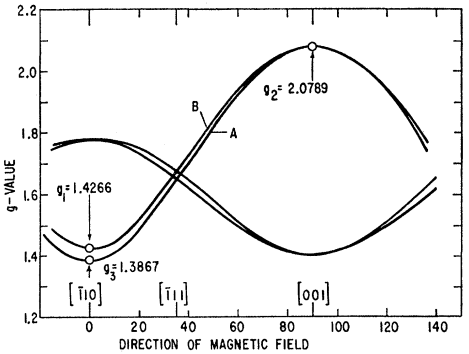

FIG. 5. The g factor of the Pt(I)$^-$ center for the magnetic field in the (110) plane. A and B are described by (7) and (6), respectively.

[15] This effect was first observed by the authors for the Ni^- center in Ge (unpublished). Similar effects have been reported by G. D. Watkins and J. W. Corbett, Phys. Rev. **121**, 1001 (1961).

[16] W. W. Tyler and H. H. Woodbury, Phys. Rev. **96**, 874 (1954).

Ni is an interstitial donor having a different type of spectrum. Third, impurity pairing between Pt and interstitial transition metal ions has been detected. Such pairs have been interpreted in terms of the acceptor ion (Pt) being substitutional.[7]

The resonance parameters indicate that the Pd ion in the Pd^- center and the Pt ion in the $Pt(I)^-$ center are distorted from the normal substitutional position. Several different models are consistent with the experimentally determined principal axes. One model is that the impurity has a d^8 configuration and completes the tetrahedral bonding with its four nearest neighbors, but there is a bound hole in a $j=\frac{3}{2}$ state localized about the impurity ion. E. O. Kane considered such a model for Ni^- in Ge, and showed that it can lead to a Jahn-Teller distortion in a [001] direction.[5]

Another model is that the impurity forms bonds with two of its four silicon nearest neighbors, as does oxygen in the Si-A center, which has the same principal axes.[17,18] In this model, the other two silicon nearest neighbors bond to each other. One then has two possibilities: the impurity might have the d^8 configuration, which is assumed to be diamagnetic, while, as in the Si-A center, the unpaired electron occupies the antibonding orbital of the two paired Si atoms. Alternatively, the impurity configuration could be d^9. There are differences between the spectra of the Pd^-[or $Pt(I)^-$] center and the Si-A center which favor the latter alternative: (1) In the Si-A center the angle between the axes of the Si^{29} interaction is less than the normal tetrahedral angle, while in the Pd^- center it is greater. (2) Upon application of a uniaxial stress, the intensities of the resonance lines of the Si-A center and the Pd^- center change in opposite directions. (3) The magnitude of the interaction with Si^{29} is only $\frac{1}{3}$ as great for the Pd^- center as for the Si-A center. (4) The hyperfine interaction with Pd^{105} is reasonably large, while the model for the Si-A center leads to zero contact interaction with a nucleus in that position. The last two points indicate that the unpaired electron is more localized on the impurity atom in the Pd^- center than one expects from the Si-A center model.

[17] G. D. Watkins and J. W. Corbett, Phys. Rev. **121**, 1001 (1961).

[18] A. D. Liehr has independently suggested a similar model in informal discussions.

ACKNOWLEDGMENT

The authors thank G. D. Watkins for discussions and C. R. Trzaskos for assistance in the measurements.